

Symmetry effects on spin switching of adatoms

C. Hübner¹, B. Baxevanis¹, A. A. Khajetoorians² and D. Pfannkuche¹

¹*Institute for Theoretical Physics, Hamburg University, Germany*

²*Institute of Applied Physics, Hamburg University, Germany*

(Dated: January 18, 2023)

Abstract

Highly symmetric magnetic environments have been suggested to stabilize the magnetic information stored in magnetic adatoms on a surface. Utilized as memory devices such systems are subjected to electron tunneling and external magnetic fields. We analyze theoretically how such perturbations affect the switching probability of a single quantum spin for two characteristic symmetries encountered in recent experiments. For a system with three-fold symmetry, which is protected against surface induced spin flips, we find a strong sensitivity to weak symmetry breaking. Further we illuminate how the switching of an adatom spin exhibits characteristic behavior with respect to low energy excitations from which the symmetry of the system can be inferred.

Recently, single magnetic atoms on surfaces, or so-called magnetic adatoms, have gained a lot of interest for spin-based information storage and processing [1, 2, 3]. These concepts are mostly based on strong magnetic anisotropy energy [4, 5], which reduces spin degeneracy at zero magnetic field, thereby defining preferential spatial orientations of the spin. While magnetic anisotropy introduces an energy cost for magnetization reversal, countless studies have illustrated that in the presence of strong magnetic anisotropy, individual magnetic adatoms still exhibit rather short lifetimes [6, 7, 8] owing to the interplay of the hybridization of the moment bearing 3d orbitals and the underlying substrate. Such observations question the role of both tunneling electrons as well as substrate electrons in dynamical processes of the atomic spin [9, 10, 11, 12, 13, 5]. In order to enhance the dynamic stability of such adatoms, strong magnetic coupling between individual spins can be utilized to protect the total spin from fluctuations which destabilize the moment [2, 14].

A different approach, that stabilizes a single magnetic moment of an adatom, was utilized by a particular choice of both spin and underlying substrate symmetry [3]. In particular for a three-fold symmetric system with the net magnetic moment $S = 8$ of a holmium adatom, it is possible to protect the spin, in the absence of perturbations, from single electron processes which can induce reversal due to for example spin-flip induced

quantum tunneling or spin-flip scattering. It is unclear how perturbations, like current-based read out or static magnetic fields which break the symmetry of the system, effect the symmetry-driven stability of the spin in such quantum systems.

Here we theoretically investigate how external perturbations modify the dynamics of a single spin in a magnetic environment with different symmetry. We extract the effective switching rate between the high-spin ground states via all possible spin paths, as experimentally manifested in two-state telegraph noise, utilizing a master equation approach. With comparative analysis we show how a single spin on both two-fold and three-fold symmetric substrates [15] responds to temperature, external magnetic field, as well as tunneling electron energy. We find that the three-fold symmetric system is highly sensitive to external perturbations since they open low energy paths for spin switching between the ground states. Although spin-flip processes are always possible for the two-fold symmetric system, their dependence on external fields is much weaker.

Such different behavior can be attributed to the symmetry dependent interaction with the underlying crystal field. By expanding the crystal field in terms of spherical harmonics, the interaction with the net spin $\hat{\mathbf{S}}$ of magnetic atoms or clusters can be expressed by various power of spin operators, the so-called Stevens operators [16]. To leading order, the spin Hamiltonian (\hat{H}_χ) can be described by a uniaxial anisotropy term proportional to \hat{S}_z^2 and multiaxial terms which are proportional to powers of the raising/lowering operators, $\hat{S}_{+/-}$. In the following the index $\chi \in \{\phi, \psi\}$ is used to label the two-fold and three-fold symmetric Hamiltonian respectively, and we use Δ_{01}^χ to denote the first excitation energy at zero magnetic field. For two-fold symmetry, which we refer to as ϕ , we can write

$$\hat{H}_\phi = D_\phi \hat{S}_z^2 + \tilde{B} \hat{S}_z + E_\phi (\hat{S}_+^2 + \hat{S}_-^2) \quad (1)$$

where D_ϕ is the uniaxial anisotropy, $\tilde{B} = \mu_B g B / \hbar$ the Zeeman energy and E_ϕ the biaxial or transversal anisotropy. The biaxial anisotropy term is the lowest order contribution leading to mixing of \hat{S}_z eigenstates. Eigenstates $|\phi_i^s\rangle$ of \hat{H}_ϕ can be separated in two subgroups $s \in \{+, -\}$, where i is the label within these group. For a half integer spin they are either a linear combination of \hat{S}_z eigenstates $|S - 2n\rangle$ forming the states $|\phi_i^+\rangle$ or $| - S + 2n\rangle$ forming $|\phi_i^-\rangle$ [17] with n being an integer. We choose a half integer spin number $S_\phi = 15/2$ for the two-fold symmetric system motivated by a Fe cluster on Cu(111) substrate [14]. For $D_\phi < 0$ all eigenstates align along an inverted parabola as depicted in Fig. 1(a) where the two subgroups

of eigenstates are explicitly differentiated by color. Due to Kramers theorem [18, 19], direct tunnel coupling between the ground states is forbidden such that $\langle \phi_0^\pm | \hat{S}_z | \phi_0^\mp \rangle = 0$. A single electron on the other hand can induce a transition between the ground states, since for example the matrix element $\langle \phi_0^+ | \hat{S}_+ | \phi_0^- \rangle$ gives a non-zero value at zero magnetic field and is proportional to $(E_\phi / |D_\phi|)^7$, as depicted in the upper inset of Fig. 1(d), which can be attributed to the mixing of \hat{S}_z eigenstates by biaxial anisotropy. With increasing magnetic field $|\tilde{B}|$ the probability for the ground state transition induced by a single electron increases further, as shown in Fig. 1(d).

For three-fold symmetry, which we refer to as ψ , we can write,

$$\begin{aligned} \hat{H}_\psi &= D_\psi \hat{S}_z^2 + \tilde{B} \hat{S}_z \\ &+ E_\psi \left(\hat{S}_z (\hat{S}_+^3 + \hat{S}_-^3) + (\hat{S}_+^3 + \hat{S}_-^3) \hat{S}_z \right). \end{aligned} \quad (2)$$

Here we include only the lowest non-vanishing order of multiaxial anisotropy, which we refer to as the hexaxial anisotropy quantified by its coefficient E_ψ . The eigenstates $|\psi_i^s\rangle$ divide in three subgroups $s \in \{+, -, 0\}$ for an integer spin and can also be expanded in \hat{S}_z eigenstates. States $|\psi_i^+\rangle$ have only contributions from $|S-3n\rangle$ and $|\psi_i^-\rangle$ only from $|-S+3n\rangle$ with an integer n . To $|\psi_i^0\rangle$ all states $|3n\rangle$ contribute with the integer $-S/3 \leq n \leq S/3$. The states are shown color coded in Fig. 1(b) for $D_\psi < 0$. Unlike the two-fold case, there is a class of eigenstates ψ_i^0 which form "within" the potential barrier meaning $\langle \psi_i^0 | \hat{S}_z | \psi_i^0 \rangle = 0$ and show tunnel splitting at zero magnetic field. With a spin number $S_\psi = 8$, as motivated by the Ho adatom on Pt(111) [3], direct tunneling between the ground states is avoided. In contrast to ϕ , single electron induced tunneling between ground states is forbidden if the spin is not an integer multiple of 3 i.e. the symmetry of \hat{H}_ψ . Without breaking time-reversal symmetry the matrix elements $\langle \psi_0^\mp | \hat{S}_+ | \psi_0^\pm \rangle = \langle \psi_0^\mp | \hat{S}_- | \psi_0^\pm \rangle$ vanish [3]. As a result, the symmetry of the system protects a given ground state spin from reversal due to single electron fluctuations which is the distinguishing feature of \hat{H}_ψ as compared to \hat{H}_ϕ . To investigate the stability of this symmetry related protection, we apply a ubiquitous magnetic field which breaks the crystal field symmetry. Fig. 1(d) shows the increasing probability for switching between the ground states with a single electron with respect to the magnetic field, even in the presence of a small field. The linear increase of switching probability for small magnetic fields is depicted in the lower inset of Fig. 1(d) and defines the lower boundary for the switching probability at finite magnetic field. As compared to the quadratic dependence of the biaxial case, this linear behavior witnesses a much stronger

sensitivity and a breakdown of the symmetry protection. This needs to be considered if a tip stray field or neighboring magnetic atoms are present in a spintronic device.

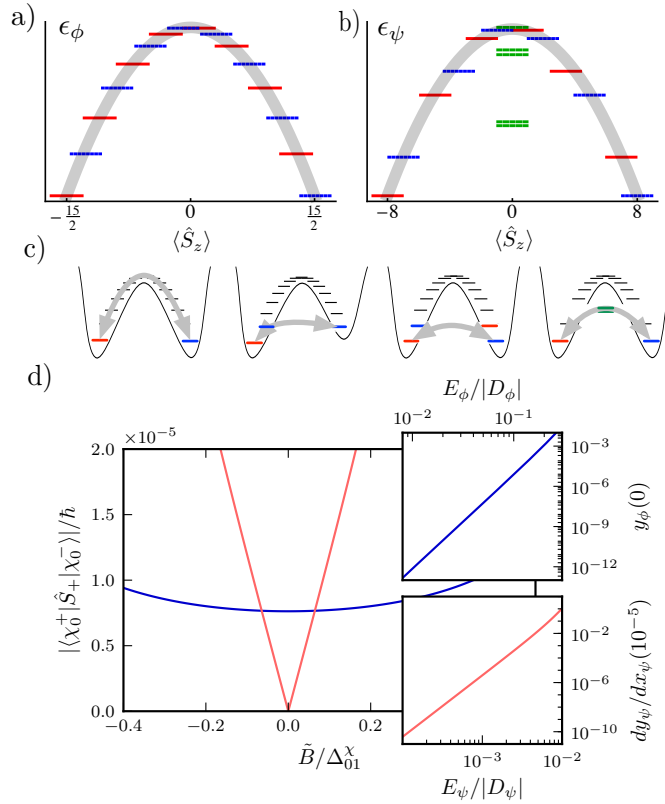


Figure 1: (color online). Energy levels of \hat{H}_ϕ (a) and \hat{H}_ψ (b) as a function of the expectation value $\langle \chi_i^s | \hat{S}_z | \chi_i^s \rangle$. The parabola indicates the anisotropy barrier. The red, green, and blue lines indicate $s = -$, $s = +$, $s = 0$ respectively. (c) The different possible paths for spin reversal are illustrated, namely from left to right electron induced switching, or ladder transitions over the barrier, quantum tunneling of magnetization, ground state switching, and shortcut tunneling. (d) $y_\chi(x_\chi) := |\langle \chi_0^+ | \hat{S}_+ | \chi_0^- \rangle| / \hbar$, as a function of magnetic field $x_\chi := \tilde{B} / \Delta_{01}^\chi$, where $E_\phi / |D_\phi| = 0.1$ is colored blue and $E_\psi / |D_\psi| = 0.002$ red. (upper inset (d)) displays the offset of y_ϕ at $x_\chi = 0$ as a function of the biaxial anisotropy E_ϕ . (lower inset (d)) shows the linear slope of y_ψ at $x_\chi = 10^{-5}$ as a function of the hexaxial anisotropy E_ψ .

The reversal of the spin between the two ground states is induced by elastic and inelastic spin flips with conduction electrons. Having a scanning tunneling microscope in mind, the conduction electrons are generated from a spin polarized tip and a non-magnetic substrate. They interact with the spin $\hat{\mathbf{S}}$ via exchange interaction described by an Appelbaum Hamiltonian [20]

$$\hat{H}_t = \frac{1}{2} \sum_{rr'kk'\sigma\sigma'} v_r v_{r'} a_{rk\sigma}^\dagger \vec{\sigma}_{\sigma,\sigma'} \cdot \hat{\mathbf{S}} a_{r'k'\sigma'}, \quad (3)$$

with the annihilation (creation) operators $a_{rk\sigma}^{(\dagger)}$ in tip $r = T$ and substrate $r = S$ and the vector of Pauli matrices $\vec{\sigma}_{\sigma,\sigma'}$ associated with the spin of the tunneling electrons with momentum k . In a perturbative expansion up to fourth order in the coupling v_r we derive a master equation for the reduced density matrix describing changes in the occupation probability of \hat{H}_χ eigenstates. Within the rates $\mathcal{W}_{\alpha\beta}$ [17] spin exchange with conduction electrons is included. We consider the case in which renormalization of energy levels from scattering on electrons [21] can be neglected. This means the tunnel coupling has to be sufficiently small compared to the temperature. Under this condition an electron bath does not destroy the coherence between the \hat{S}_z states contributing to the $|\psi_i^0\rangle$ class. By solving the master equation we identify the dominant switching rate Γ_χ between the two polarized spin states $|\chi_0^+\rangle$ and $|\chi_0^-\rangle$. All possible paths are included in the switching rate and can be characterized as depicted in Fig. 1(c). Each path is effected differently by external perturbations such as temperature, applied voltage or magnetic field. This makes their contribution to the total switching rate Γ_χ distinguishable in specific parameter regimes. All rates will be given in units of the total spin flip rate $\Gamma_0 = \pi \hbar^2 v_T^2 v_S^2 (\rho_{T\uparrow} \rho_{S\downarrow} + \rho_{T\downarrow} \rho_{S\uparrow}) / |\mathcal{D}| (2S - 1)$ for electrons inelastically tunneling from the tip to the surface.

In order to surmount the anisotropy barrier along the spin ladder, at least $2S$ sequential spin flip processes are needed. Nevertheless, due to strong relaxation generated by substrate electrons, typically more electrons are needed. Moreover, each electron requires a minimum energy of Δ_{01}^χ , which corresponds to the excitation energy of the spin system. Such electron energies are generated either by the applied voltage eV between the tip and substrate or from temperature $k_B T$. With just uniaxial anisotropy and with small temperatures $k_B T \ll \Delta_{01}^\chi$ a threshold voltage $eV = \Delta_{01}^\chi$ denotes the onset of spin switching due to the aforementioned ladder processes as shown in Fig. 2 (bright region). The system with the larger spin ψ shows less switching, since more inelastic excitations are needed to reverse the spin due to the larger number of ladder states.

At zero voltage and constant k_bT/Δ_{01}^x temperature induced transitions between the ground and the first excited state allow switching even below the first excitation energy $eV = \Delta_{01}^x$ as depicted in Fig. 2 (greyed region). The mixing of \hat{S}_z eigenstates with multiaxial anisotropy leads to an increase of the rate between the ground and the first excited state. Additionally the energy levels of the spin states are shifted by the multiaxial anisotropy which has an effect on the rates between excited states. Especially for the system ψ the excited states $|\psi_i^0\rangle$ become accessible and establish an extra switching path that is absent in ϕ . Despite the absolute value of the switching rate Γ depending on E_ϕ/E_ψ , the characteristic behavior with respect to the voltage is similar in both systems.

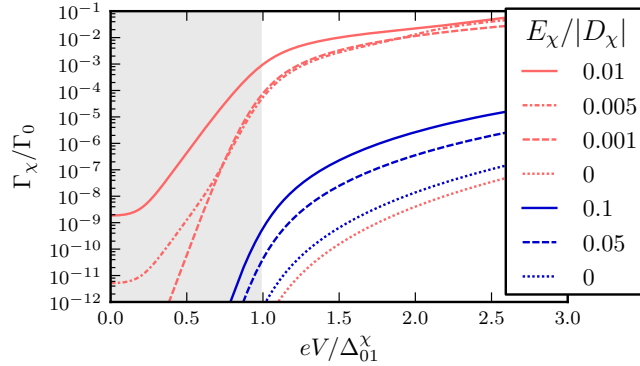


Figure 2: (color online). Switching rate Γ_χ between the ground states as a function of applied bias voltage eV between the tip and the surface. ϕ is blue and ψ is colored red. Increasing transversal anisotropy $E_\chi/|D_\chi|$ results in temperature induced excitations below the threshold voltage $eV = \Delta_{01}^x$ marked by the gray region. ($|v_T|/|v_T| = 0.15$, $\tilde{B} = 0$, $k_B T = 0.05\Delta_{01}^x$)

A single electrons that induces elastic quantum tunneling between the ground states mainly originates from the unpolarized substrate since the relative coupling $v_T/v_S \ll 1$ is much stronger. Rates between two degenerate states for an unpolarized substrate become

$$\mathcal{W}_{\chi_i^\mp \chi_i^\pm} \propto \left(|\langle \chi_i^\mp | \hat{S}_+ | \chi_i^\pm \rangle|^2 + |\langle \chi_i^\mp | \hat{S}_- | \chi_i^\pm \rangle|^2 \right) k_b T \quad (4)$$

and represent transitions due to electron-induced quantum tunneling [17]. A single electron can transfer its spin to induce a transition between the ground states. For half integer adatom spin a single electron can always

induce transitions between the two highest lying degenerate states. From the rate one can distinguish two situations for which transitions between lower lying degenerate spin states are forbidden: (i) the complete absence of multiaxial anisotropy. (ii) the symmetry of the system prohibits electron induced quantum tunneling as is the case with \hat{H}_ψ with the choice of S_ψ being not an integer multiple of three. This is exactly the observed protection of the lifetime in ref. [3].

Fig. 3 depicts the effect of electron-induced quantum tunneling on the switching rate for both systems as a function of temperature. At $k_B T > 0.15\Delta_{01}^x$, thermally induced switching over the barrier results in Arrhenius-like behavior. The largest effect of electron-induced quantum tunneling can be seen at temperatures $k_B T < 0.1\Delta_{01}^x$ (inset of Fig. 3) in which thermal excitations can be neglected for the chosen multiaxial anisotropy values and the absence of magnetic field results in the highest degree of degeneracy. For \hat{H}_ϕ multiple channels for electron induced quantum tunneling are accessible due to a finite voltage $1.5eV/\Delta_{01}^x$. For \hat{H}_ψ on the other hand electron induced quantum tunneling is forbidden due to symmetry and a plateau appears for temperatures $k_B T < 0.1\Delta_{01}^x$. This makes ψ more robust than ϕ against surface electron-induced switching in the low temperature regime and in the absence of perturbations breaking time-reversal symmetry.

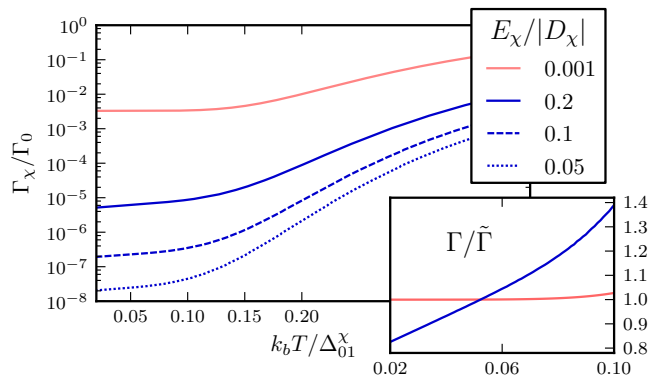


Figure 3: (color online). Temperature dependence of switching rate Γ_χ at $eV = 1.5\Delta_{01}^x$. ϕ is colored blue and ψ red. The inset magnifies the low temperature region and is normalized to $\tilde{\Gamma} = \Gamma_\chi(k_B T = 0.05\Delta_{01}^x)$. This allows a comparison of the linear behavior. ($|v_T|/|v_T| = 0.15$, $\tilde{B} = 0$)

At larger magnetic fields, namely $\tilde{B} \approx \Delta_{01}^x$, relaxation channels via tunnel mixed spin states open resulting from quantum tunneling of magnetiza-

tion [22]. A finite E_χ is needed in order to obtain this mixing. The stronger the mixing the more robust is the relaxation channel against variation of the magnetic field from the resonance condition. This is manifested in Fig. 4 as peaks in the switching rate. For $E_\phi/|D_\phi| = 0.05$ eigenstates are only weakly perturbed \hat{S}_z eigenstates, however at $|\tilde{B}| = \Delta_{01}^\phi$ all unperturbed states cross pairwise leading to an efficient mixing in the presence of finite E_ϕ . \hat{H}_ϕ has the strongest mixing between spin states at the top of the barrier.

The largest contribution to switching via quantum tunneling of magnetization in \hat{H}_ψ results from mixing of spin states in the valley of the barrier namely $|\psi_0^\pm\rangle$ and $|\psi_1^\mp\rangle$, if $|\psi_0^\mp\rangle$ is the ground state. For $E_\psi/|\Delta_{01}^\psi| = 0.01$ a single resonant tunneling channel emerges at $|\tilde{B}| \approx 1.2\Delta_{01}^\chi$. Since for $E_\psi/|D_\psi| = 0.01$ the hexaxial anisotropy already shifts the energy levels resonance condition occur at different magnetic fields. This leads to a sequence of single channel opening for relaxation. Lowering the anisotropy to $E_\psi/|D_\psi| \rightarrow 0.002$ has two effects: (i) the resonance peaks from quantum tunneling of magnetization shift to the resonance condition of the unperturbed system $|\tilde{B}| = \Delta_{01}^\chi$. (ii) an underlying substructure becomes visible with a central resonance peak that can be related to inelastic electron induced short cut tunneling created by states from the subgroup $|\psi_i^0\rangle$ as depicted in Fig. 1(c). The side peak at $|\tilde{B}| \approx 1.2\Delta_{01}^\chi$ comes from a short cut that is reestablished with magnetic field.

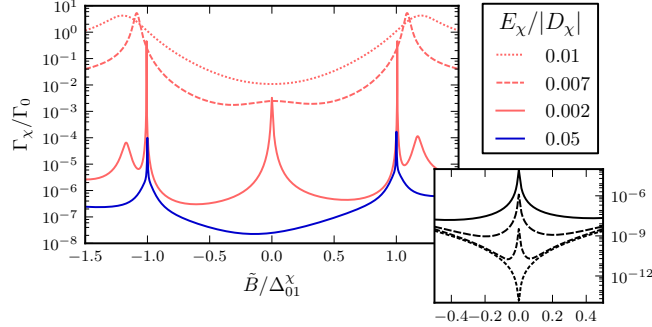


Figure 4: (color online). Switching rate Γ_χ in dependence of magnetic field at $eV = 1.5\Delta_{01}^\chi$ and $k_bT = 0.05\Delta_{01}^\chi$. ϕ is colored blue and ψ is red. For \hat{H}_ψ the transversal anisotropy is changed and shows three resonances in the range of the magnetic field. The center resonance becomes visible at $E_\psi/|D_\psi| < 0.01$ and is a result of short cut tunneling. The narrow resonance belongs to quantum tunneling of magnetization and shifting from $|\tilde{B}|/\Delta_{01}^\chi \approx 1.2$ to 1.0 with the change of hexaxial anisotropy. The broad side peak is due to restored short cut tunneling by magnetic field. The inset magnifies shows the switching rate as a function of magnetic field for ψ at $E_\psi/|D_\psi| = 0.002$ with decreasing voltage $eV/\Delta_{01}^\chi \in \{1, 0.8, 0.6, 0.2\}$ in decreasing order of the rate. The tip polarization is 10%.

The inset of Fig. 4 shows the disappearance of the central resonance from short cut tunneling at small voltages. If the electron energy as a combination of voltage and temperature exceeds the threshold Δ_{01}^ψ inelastically scattering electrons can lead to the first and second excitation and thus switching becomes effective through the shortcuts. Below the threshold voltage and with exponentially suppressed thermal excitations the switching rate goes to zero since the ground state switching is prohibited by symmetry. In the case of ϕ the rate would not go to zero since electron induced ground state switching is always present. A finite magnetic field destroys the time-reversal symmetry and thus an increasing switching rate is observable if excitations are suppressed. Above the threshold voltage the switching rate Γ decreases with magnetic field since the eigenstates $|\psi_i^0\rangle$ of \hat{H}_ψ become well separated on both sides of the anisotropy potential and the short cut is closed.

In conclusion we compared the qualitative behavior of the switching rate between two polarized states of a single spin in a two- and three-fold symmetric system with respect to external perturbations such as magnetic field, temperature and spin excitations due to conduction electrons. We found

that the protection against ground state transitions, induced by a single electron, in the three-fold symmetric system can be destroyed by a magnetic field. This makes the switching more sensitive to time-reversal symmetry breaking in contrast to the two-fold symmetric system. This protection also leads to a constant switching rate in the low temperature regime, which makes the symmetries distinguishable by measurement. Transitions to excited spin states, via inelastically tunneling electrons, make multiple fast paths for switching across the anisotropy barrier accessible. The three-fold symmetry provides a rapid switching through short cuts in the barrier that are missing under two-fold symmetry. This makes it possible to distinguish the symmetry by measuring the switching rate as a function of magnetic field.

We acknowledge funding through SFB925, GrK1286, SFB668, Emmy Noether KH324/1-1 and DFG. We want to thank KIT members for invitation and discussion, especially Christian Karlewski, Wulf Wulfhekel and Gerd Schön.

References

- [1] A. A. Khajetoorians, J. Wiebe, B. Chilian, and R. Wiesendanger, “Realizing all-spin-based logic operations atom by atom.,” *Science (New York, N.Y.)*, vol. 332, pp. 1062–4, May 2011.
- [2] S. Loth, S. Baumann, C. P. Lutz, D. M. Eigler, and A. J. Heinrich, “Bistability in atomic-scale antiferromagnets,” *Science*, vol. 335, no. 6065, pp. 196–199, 2012.
- [3] T. Miyamachi, T. Schuh, T. Märkl, C. Bresch, T. Balashov, A. Stöhr, C. Karlewski, S. André, M. Marthaler, M. Hoffmann, M. Geilhuge, S. Ostanin, W. Hergert, I. Mertig, G. Schön, A. Ernst, and W. Wulfhekel, “Stabilizing the magnetic moment of single holmium atoms by symmetry,” *Nature*, vol. 242, p. 503, 2013.
- [4] C. F. Hirjibehedin, C.-Y. Lin, A. F. Otte, M. Ternes, C. P. Lutz, B. A. Jones, and A. J. Heinrich, “Large magnetic anisotropy of a single atomic spin embedded in a surface molecular network.,” *Science*, vol. 317, pp. 1199–203, Aug. 2007.
- [5] I. G. Rau, S. Baumann, S. Rusponi, F. Donati, S. Stepanow, L. Gragnaniello, J. Dreiser, C. Piamonteze, F. Nolting, S. Gangopadhyay, O. R. Albertini, R. M. Macfarlane, C. P. Lutz, B. Jones, P. Gambardella, A. J.

- Heinrich, and H. Brune, “Reaching the Magnetic Anisotropy Limit of a 3d Metal Atom.,” *Science*, vol. 988, May 2014.
- [6] F. Meier, L. Zhou, J. Wiebe, and R. Wiesendanger, “Revealing magnetic interactions from single-atom magnetization curves,” *Science*, vol. 320, no. 5872, pp. 82–86, 2008.
- [7] A. A. Khajetoorians, S. Lounis, B. Chilian, A. T. Costa, L. Zhou, D. L. Mills, J. Wiebe, and R. Wiesendanger, “Itinerant nature of atom-magnetization excitation by tunneling electrons,” *Phys. Rev. Lett.*, vol. 106, p. 037205, Jan 2011.
- [8] A. A. Khajetoorians, J. Wiebe, B. Chilian, S. Lounis, S. Blügel, and R. Wiesendanger, “Atom-by-atom engineering and magnetometry of tailored nanomagnets,” *Nat. Phys.*, vol. 8, p. 497, Apr. 2012.
- [9] C. Romeike, M. Wegewijs, and H. Schoeller, “Spin Quantum Tunneling in Single Molecular Magnets: Fingerprints in Transport Spectroscopy of Current and Noise,” *Physical Review Letters*, vol. 96, p. 196805, May 2006.
- [10] N. Lorente and J.-P. Gauyacq, “Efficient Spin Transitions in Inelastic Electron Tunneling Spectroscopy,” *Physical Review Letters*, vol. 103, p. 176601, Oct. 2009.
- [11] F. Delgado and J. Fernández-Rossier, “Spin dynamics of current-driven single magnetic adatoms and molecules,” *Physical Review B*, vol. 82, p. 134414, Oct. 2010.
- [12] A. Chudnovskiy, C. Hübner, B. Baxevanis, and D. Pfannkuche, “Spin switching: From quantum to quasiclassical approach,” *Physica Status Solidi B*, vol. 13, pp. 1–13, Apr. 2014.
- [13] N. Bode, L. Arrachea, G. S. Lozano, T. S. Nunner, and F. von Oppen, “Current-induced switching in transport through anisotropic magnetic molecules,” *Physical Review B*, vol. 85, p. 115440, Mar. 2012.
- [14] A. A. Khajetoorians, B. Baxevanis, C. Hübner, T. Schlenk, S. Krause, T. O. Wehling, S. Lounis, A. Lichtenstein, D. Pfannkuche, J. Wiebe, and R. Wiesendanger, “Current-driven spin dynamics of artificially constructed quantum magnets,” *Science*, vol. 339, no. 6115, pp. 55–59, 2013.

- [15] D. Gatteschi and L. Sorace, “Hints for the Control of Magnetic Anisotropy in Molecular Materials,” *Journal of Solid State Chemistry*, vol. 159, pp. 253–261, July 2001.
- [16] K. W. H. Stevens, “Matrix Elements and Operator Equivalents Connected with the Magnetic Properties of Rare Earth Ions,” *Proceedings of the Physical Society. Section A*, vol. 65, pp. 209–215, Mar. 1952.
- [17] *See supplemental material*, 2014.
- [18] H. Kramers, “Théorie générale de la rotation paramagnétique dans les cristaux,” *Proceedings Koninklijke Akademie van Wetenschappen*, no. 33, pp. 959–972, 1930.
- [19] M. J. Klein, “On a Degeneracy Theorem of Kramers,” *American Journal of Physics*, vol. 20, no. 2, p. 65, 1952.
- [20] J. Appelbaum, “Exchange Model of Zero-Bias Tunneling Anomalies,” *Physical Review*, vol. 154, pp. 633–643, Feb. 1967.
- [21] J. C. Oberg, M. R. Calvo, F. Delgado, M. Moro-Lagares, D. Serrate, D. Jacob, J. Fernández-Rossier, and C. F. Hirjibehedin, “Control of single-spin magnetic anisotropy by exchange coupling,” *Nature nanotechnology*, vol. 9, pp. 64–8, Jan. 2013.
- [22] D. Gatteschi, R. Sessoli, and J. Villain, *Molecular Nanomagnets*. Oxford Univ. Press, Oxford, 2006.